RESEARCH EXPERIENCE OF AEROELASTIC VIBRATIONS OF THE UFV WITH ELECTROMECHANICAL ACTUATOR OF CONTROL FIN

Vsevolod I. Smyslov[1], Artyom V. Bykov[1], Stanislav I. Sychev[2]

[1] Aeroelasticity Department, TsAGI
Zhukovsky str. 80, Zhukovsky, Moscow Region, Russia, 140180
smysl@mail.ru, a.bykov@list.ru

[2] Tactical Missiles Corporation
7 Ilicha Str., Korolev, Moscow Region, Russia, 141075
sychevsi@gmail.com

Keywords: flutter, elastic UFV–CS loop, electromechanical actuator, auto-oscillations.

Abstract: Features of considered unmanned flight vehicle (UFV), which define the method of research of flutter and stability of "elastic UFV – control system (CS)", are shown. Main stages of experimental and computational efforts for preventing dangerous auto-oscillations in flight are presented. The usage of digital CS along with high performance actuators makes experimental works more complex and requires a lot of modification of test object to carry out the stand tests. Frequency method of estimating the stability and limited-cycle loop (LCO) amplitude required to obtain in experiment a multitude of measurements of combinations of frequency responses functions (FRF) of separate elements of "elastic UFV–CS" loop. These data for stability evaluation are complemented by computational aerodynamic characteristics. Results of experimental tests are given.

1 Introduction

The most important task of dynamic aeroelasticity is preventing the UFV dangerous auto-oscillations in flight [1-3]. Auto-oscillations can lead to structure damage, malfunction or failure of UFV subsystems.

Main phenomena to be addressed are flutter and instability of "elastic UFV – CS" loop, or stabilization loop, at frequencies of natural oscillations. The solution for the task consists of determining of stability boundary and analysis of aeroelastic behavior near the boundary.

All amount of operating conditions could be covered by computation only, the reliability of computation is based on results of ground stand tests. Therefore the combined usage of computational and experimental methods is a main feature.

The discussed topic is UFV of cross-shaped type ("+" or "X"), with construction of control fins of low or extra-low aspect ratio. Flight regimes include both sub- and supersonic. Every control fin has individual electromechanical actuator (except UFV of canard type with paired control fins). There are three independent circuits in CS (pitch, yaw and bank channels).

Due to relatively small sizes and weight the natural frequencies are high and amplitudes are small, which makes measurements difficult.

The structure multi variance and modularity with asymmetry of elastic-inertial parameters in control planes and nonlinearity of stiffness significantly increase summary duration of test.

Usage of high-performance electromechanical actuator with small allowed continuous operating time, resource and large discrepancy in characteristics (FRF, for example) cause complications in experiment and further analysis of aeroelastic stability. Practice of wind tunnel tests of UFV for aeroelastic tasks lacks due to certain reasons.

2 TEST SEQUENCE, FLUTTER, UFV–CS LOOP

The sequence of computational and experimental works is defined by work sequence, creation of pilot sample (prototype).

The initial stage of works includes preliminary flutter computations on base of CAD models, which give common headlines for further flutter analysis – typical outcome result is shown on (Figure. 1).

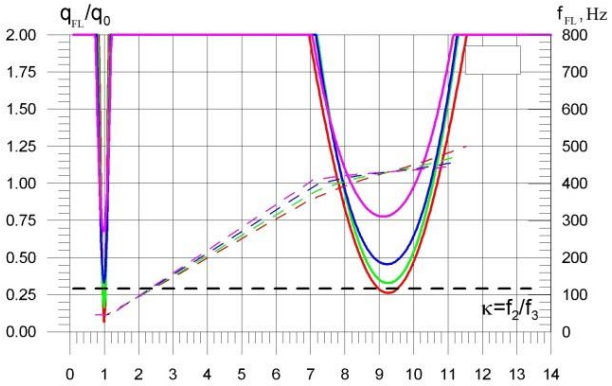

Figure 1: Standard dependence of q_{FL} and f_{FL} from rotation frequency at M=const
f_2 – frequency of rudder rotation; f_3 – frequency of the 1st body bending

According to that sequence, the manufacturing of first control fin samples allows to provide modal tests (to determine natural frequencies and mode shapes) of cantilever-type fixed control fin (Figure. 2). This is necessary for FEM model updating (tuning). In addition computations give aerodynamic derivatives in function of Mach number M, used both for flutter and stability analysis of "elastic UFV – CS" loop.

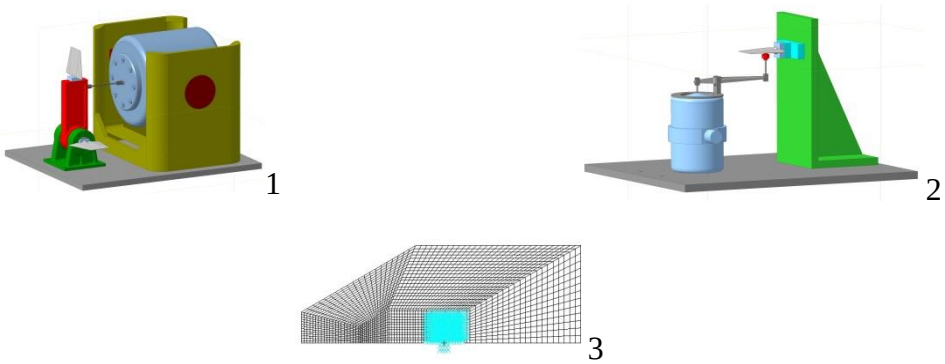

Figure 2: Cantilevered control fin. Experimental scheme of excitation:
1) kinematic; 2) by force; 3) FEM model for the determination of $\mathbf{C_y^\alpha}$

After manufacturing of first samples of actuator compartment the tests are carried out in static position to get actuator FRF and amplitude responses (AR) which may be useful, though they may be not feasible. This data could define more exactly the amount of future tests and update preliminary flutter boundaries.

The main work starts with whole UFV pilot sample with equipment modified for ground stand tests. Auxiliary equipment (providing UFV operating in "flight" mode) should be supplied too. Ground vibration tests (GVT) and FRF measurements of "elastic UFV – CS" loop parts are carried out. The results of it allow to update computational models of flutter and stability analysis of "elastic UFV – CS" loop. Known expression of oscillations

$$C\ddot{q} + H\dot{q} + Gq + (v^2Bq + vD\dot{q}) = 0 \quad (1)$$

(where q is a generalized (in Lagrangian approach) coordinate; C, H, D, G, B are matrices of inertia, structure and aerodynamic damping, structure and aerodynamic stiffness) could be reduced (in case of stand test at stability boundary) to equation of harmonic oscillations

$$C\ddot{q} + H\dot{q} + Gq = A\cos(\omega t) \quad (2)$$

where A is a matrix with elements of CS. Flutter task, as more particular, will differ from (2) by a zero right part. The task of loop stability contains the cinematic excitation in right part, depending on structure oscillations.

In practice the first problem solution (where right part is 0) is completed by eigenvalues computation, and the second task – by frequency hodograph and Nyquist criterion [4]. Both methods use a same structure model and are based on same (as a rule) aerodynamic theory.

Unlike flutter, the additional measurements of FRF are required (as minimum, for UFV body and for some points in chain of CS circuit parts) for frequency hodograph method. Nonzero right part leads to increasing of amount of tests.

The more general approach is associated with computation of oscillations in subcritical area, for example, by root tracks (hodograph) against dynamic pressure in flutter task, and in some cases, in overcritical area (for LCO analysis).

Hodograph computations require to analyze multiple variants for many frequencies and for different flight conditions.

3 STAND EXPERIMENT FOR NATURAL OSCILLATIONS MEASUREMENT

In case of UFV the GVT are based on traditional approach, in which expression (2) contains in right part force vector $F\cos(\omega t)$ with 1 – 4 non-zero elements. The tests are carried out in a known way (Figure. 3) with electrodynamic (modal) exciters in some points and using up to 20-30 accelerometers. The object is suspended by elastic cords in two points, close as much as possible to nodes of 1-st bending mode. The interaction of suspended as rigid object "zero" modes (usually 2-4 Hz), on elastic modes (40-80 Hz) is excluded. The tests are carried out (repeated) for some UFV orientation (2-4), because structure asymmetry (fuselage spine fairing, access hatches) leads to difference of stiffness characteristics in different planes.

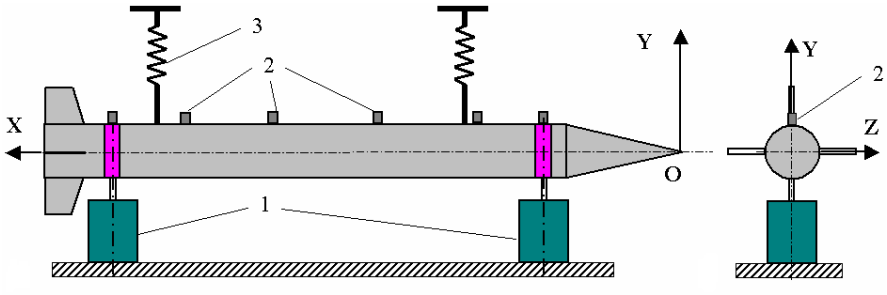

Figure 3: A typical scheme of the experiment: 1- exciters, 2 - accelerometers, 3 - elastic suspension

The common volume of tests consists of measurement of real (synphase to excitation) and imaginary (shifted by quarter period) parts of main harmonic of excitation signal in range of first 3-5 elastic natural modes. As a rule, the form of measured signal, especially on high frequencies is far from sinusoidal.

In addition, the impact tests are used for estimating of amplitude spectrum in frequency range of interest.

Main part of tests are carried out with non-operating actuators (set on arrester), however some measurements require the actuators to be powered on (without controlled signals input). The permitted duration (by thermal conditions) of such measurements can be 20-30 seconds and decreases dramatically with frequency grow, which significantly rises the total test time.

The results of ground tests are used for updating of parameters of computational dynamical scheme of structure. This data is used for multi-parameter computation of flutter.

4 ELECTROMECHANICAL ACTUATOR AND UFV MODIFICATION

Unlike pneumatic or hydraulic actuator, the electrodynamic actuator (Figure 4) includes a complex mechanical part – a gearbox. The mathematical description of such object could not be reduced to single degree of freedom (DOF), or to single-mass model. Principal design could be various (gear system, ballscrew-nut transmission, e.tc.), but in any case the transmission coefficient is large, approximately in a range of 150-200.

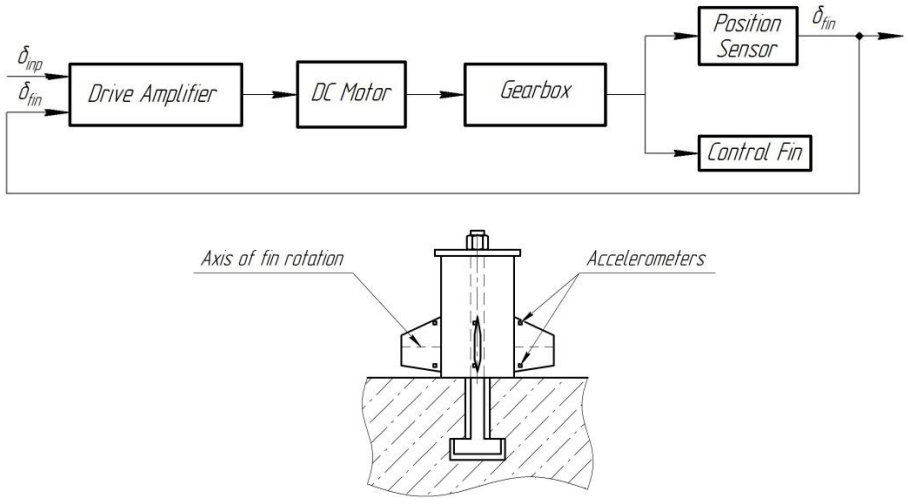

Figure 4: Electromechanical actuator: block diagram and control fin actuation system

The presence of amplitude response (AR) nonlinearity (due to freeplays and friction) and, thereby the dependence on frequency requires to measure AR's on some frequencies, close to body natural frequencies, [5] Figure. 5. On basis of AR data the amplitude selection is made for FRF measurement (according to maximal ratio of output signal amplitude to input, Figure. 6). In order to decrease the influence of backlash the harmonic low frequency component is added to exciting signal.

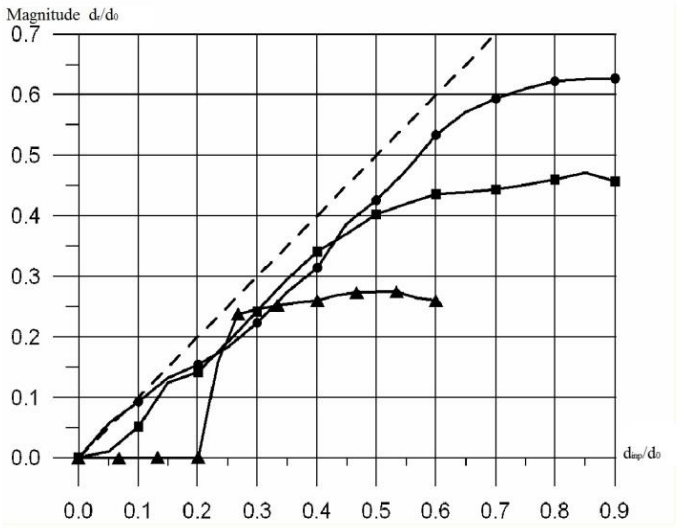

Figure 5: Experimental amplitude response (AR) of electromechanical actuator
● – *f*=30 Hz, ■ – *f* =45 Hz, ▲ – *f* =80 Hz

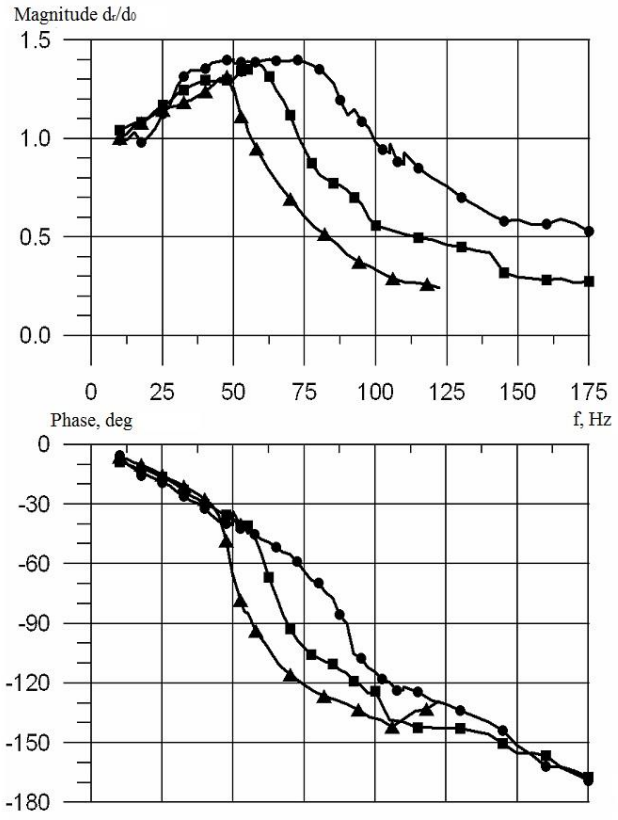

Figure 6: Experimental FRF of electromechanical actuator
● –δ_{inp}=0.2 deg.,■ – δ_{inp} =0.35 deg.., ▲ – δ_{inp} =0.6 deg.

For problems of flight dynamics (frequencies below 10 Hz), the characteristics of actuator are strictly regulated by developer, therefore the different actuator samples have close characteristics from one sample to next one. However such stability or standard is not guaranteed for aeroelastic frequencies (and this is difficult to realize) and actuators have FRF with significant discrepancies, which can be obtained by experimental way only.

UFV modifications for test mentioned above include enabling access to actuator's inputs, outputs (feedback signals), making possible independent (self-contained) operation of actuators and CS (Figure 7).

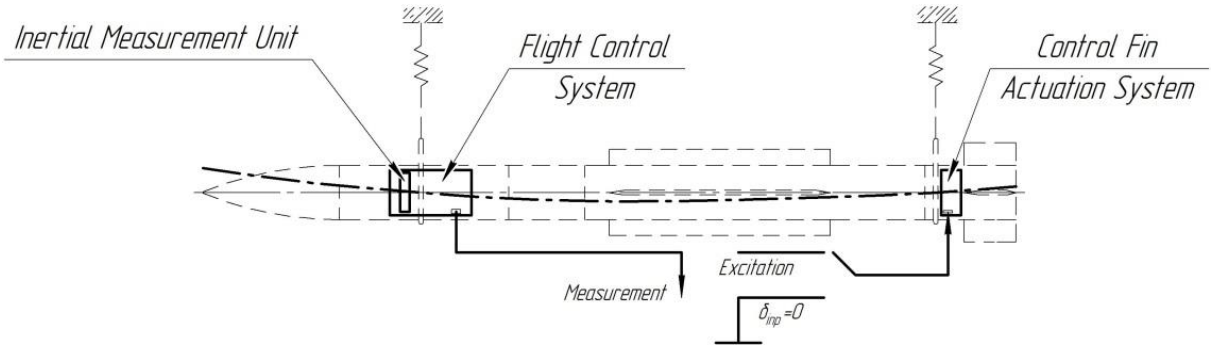

Figure 7: UFV modifications

CS is modified with objective to disable integrating units, to introduce experiment with variable (adaptive) coefficients in according to some Mach number, speed and altitude ("frizzed" regime). The other important modification allows to measure CS sensors signals directly at CS analog outputs.

5 ELASTIC UFV-CS LOOP, PARTS CHARACTERISTICS

Typical block diagram of stabilization loop channel (pitch or yaw) for a UFV with an analog control of actuation system for research of stability, can be represented by the example shown in Figure 8. Elastic vibrations are taken by the body and measured by analog or digital sensors: angular velocity sensor (AVS) and linear acceleration sensor (LAS).

Signals are sent in the algorithmic part of the stabilization system through the interface converter (e.g., through pulse-frequency converters in the case of digital sensors) comprising a system of variable coefficients – adaptation coefficients (which depend, in general, from the flight parameter M and q), as well as integration units, limiter units and other.

The command signal formed as a result of the algorithmic part passes through the correction filter (if it is implemented as a program) and then supplied to the digital-analog converter (DAC). The signal on the control fin actuator causes rotational vibrations of control fin, which can excite body vibrations (through stream and by inertial forces).

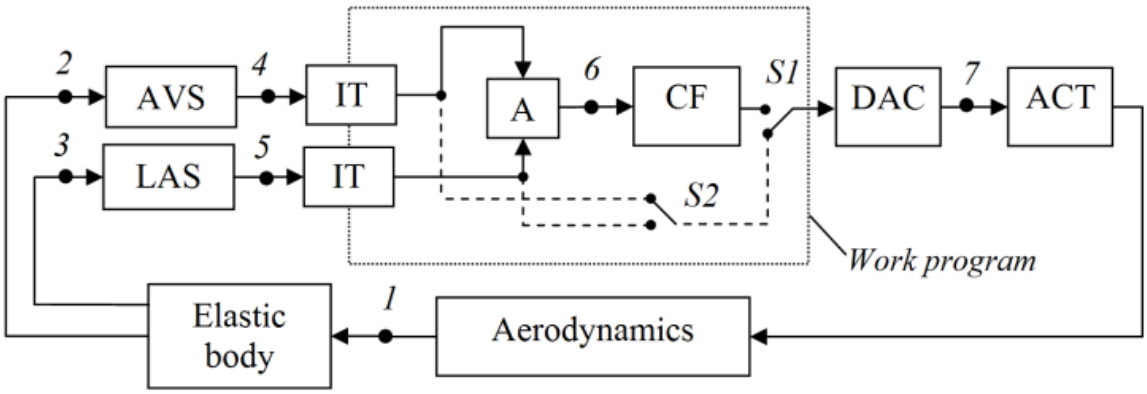

a)

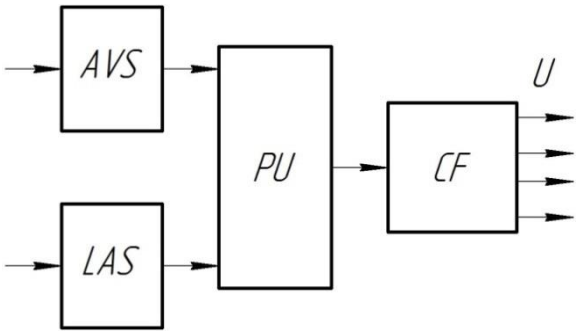

b)

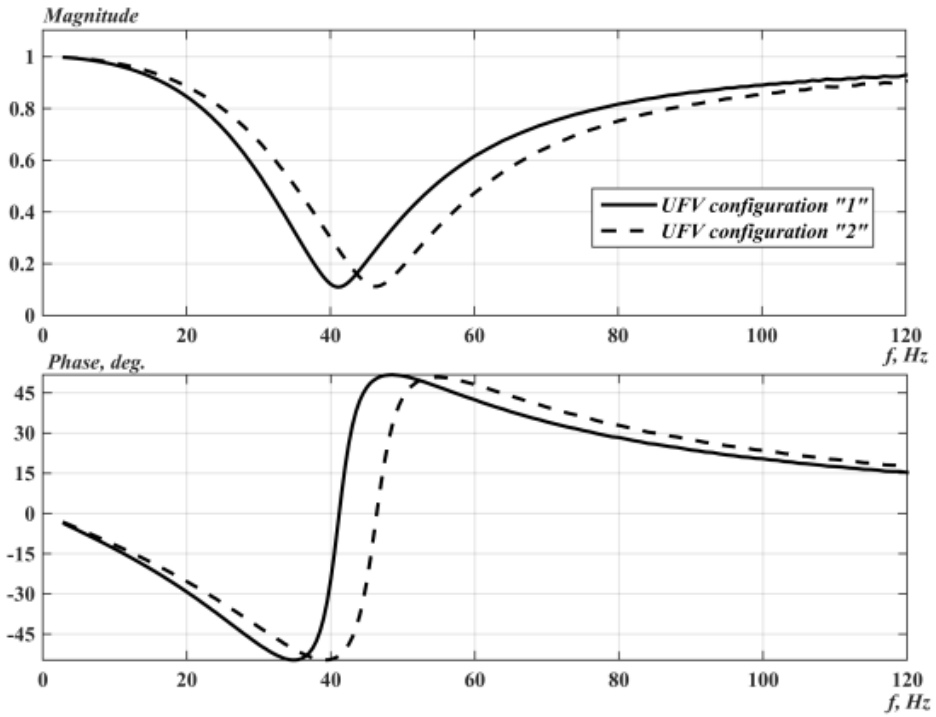

c)

Figure 8: Block diagram of stabilization loop. IT – interface transformer, A – algorithm, PU – processing unit.

The transfer function of a full open loop for the angular speed, W, is expressed as the product of

$$W = W_b \cdot W_{AVS} \cdot W_i \cdot W_A \cdot W_F \cdot W_{DAC} \cdot W_d \cdot K_a \quad (3)$$

which includes the following transfer functions:

- W_b – from force applied to control fins (or body in that section) to body angular velocity in AVS and LAS position (from point 1 to point 2 in Fig. 8)
- W_{AVS} – sensor transfer function
- W_i – interface converter transfer function
- W_A – algorithmic part by the angular velocity
- W_F – transfer function of correction filter
- W_{DAC} – DAC transfer function
- W_d – control fin actuator transfer function
- $K_a = C_y^\delta Sq$ – aerodynamic coefficient of control fin force per one angle degree, C_y^δ – derivative of lift by angle of the control fin depending on Mach number, S – characteristic area, q – dynamic pressure.

The system of variable coefficients can be simulated numerically using data provided by CS developer due to complexity of its experimental study. Nonlinear units are replaced by their linear equivalents. Regarding the interested level of vibrations, several equivalent units can be used for different levels.

The most dangerous flight modes (in terms of aeroelastic stability) are determined by the maximum value of coefficient K_a and adaptation factor product (W_A). These maxima do not correspond to the maximum of dynamic pressure at all.

One option of study is carried out on the UFV with a modified CS (work program is modified), that transfers a signal from AVS and LAS directly to the actuation system analog inputs. The algorithmic part of the CS and the filter are set to unit (1,0) to increase the signal level and improve quality of measurements. Figure 8 shows the dotted lines as data path after modofication. The experimentally measured FRF from point 1 to point 7 corresponds to the transfer function

$$W_F = W_b \cdot W_{AVS} \cdot W_i \cdot W_{DAC}. \quad (4)$$

Thereby the transfer function of the full open loop is obtained as:

$$W = W_F \cdot W_d \cdot W_A. \quad (5)$$

In case the filters are implemented as part of the work program, they are described by discrete equations with the coefficients calculated by the continuous model. For example there are two sets of coefficients for the "empty" (with “burnt-out” engine) and "charged by fuel" (start engine option) configuration. It is also possible to make a "continuous" change of filter parameters in line with 1st bending mode frequency change during an engine operation.

Figure 8.c shows the computed filter FRF for two body configurations, designated, respectively, №1 and №2. The data is obtained by the "virtual measurements" of the discrete filter model by passing through the test model of the sinusoidal signal. The results indicate the

effects of sampling (irregularity of amplitude and phase), and singularity at half of sampling frequency (not shown).

The equation of loop oscillation in flight differs from (1) by right part:

$$C\ddot{q} + H\dot{q} + Gq + (v^2Bq + vD\dot{q}) = a_1\omega_z + a_2n_y \quad (6)$$

where coefficients a_1 and a_2 depend on adaptation coefficients – K_ω and K_n, which depend, in general, on the Mach number and dynamic pressure q. At the stand v=0, and the oscillations are excited by forces applied to the control fin or the body in a section of rotation axis. As a counter example to the above, the oscillations are measured in the body section, where CS sensors are located.

There are 5 modes of measurement: 1- AVS signal, 2 – LAS signal, 3 – AVS signal through algorithmic part, 4 – LAS signal through algorithmic part, 5 – sum 3+4. The corresponding equations are

$$C\ddot{q} + H\dot{q} + Gq = F\cos(\omega t) + L; L = [\omega_z; n_y; a_1\omega_z; a_2n_y; a_1\omega_z + a_2n_y]^T \quad (7)$$

where T – is a sign of transposition. Thus, the CS adaptation coefficients may be considered or not considered in the measurement process and the actual effect of correcting filters could be estimated.

Figure 9 shows FRF of CS sensors signal and body angular velocity from force applied to the fin rotation axis. An additional characteristic, enabling to control the FRF calculation for the UFV (based on mathematical model updated according to the GVT) is the dependence of body angular velocity or linear acceleration (in a CS sensor section) on the body excitation force. It helps to clarify the effect of body structure damping.

One of the main FRF is the response from force applied to body to actuation system inputs, see equations (4). They allow to take into account elasticity of joints between CS sensors and body, the impact of side resonances, if any, and other effects. Figure 10 is an example of such CS characteristics of an angular velocity chain in case of circuit acceleration circuit is turned off.

In ideal case of vertical excitation applied in the plane of pitch θ, the body oscillations are placed strictly in this plane and all the outputs should be the same, but it is not achieved in fact. One can see that oscillations of the body occur in two planes, and even in a roll. This motion is being caused by the asymmetry of the UFV structure.

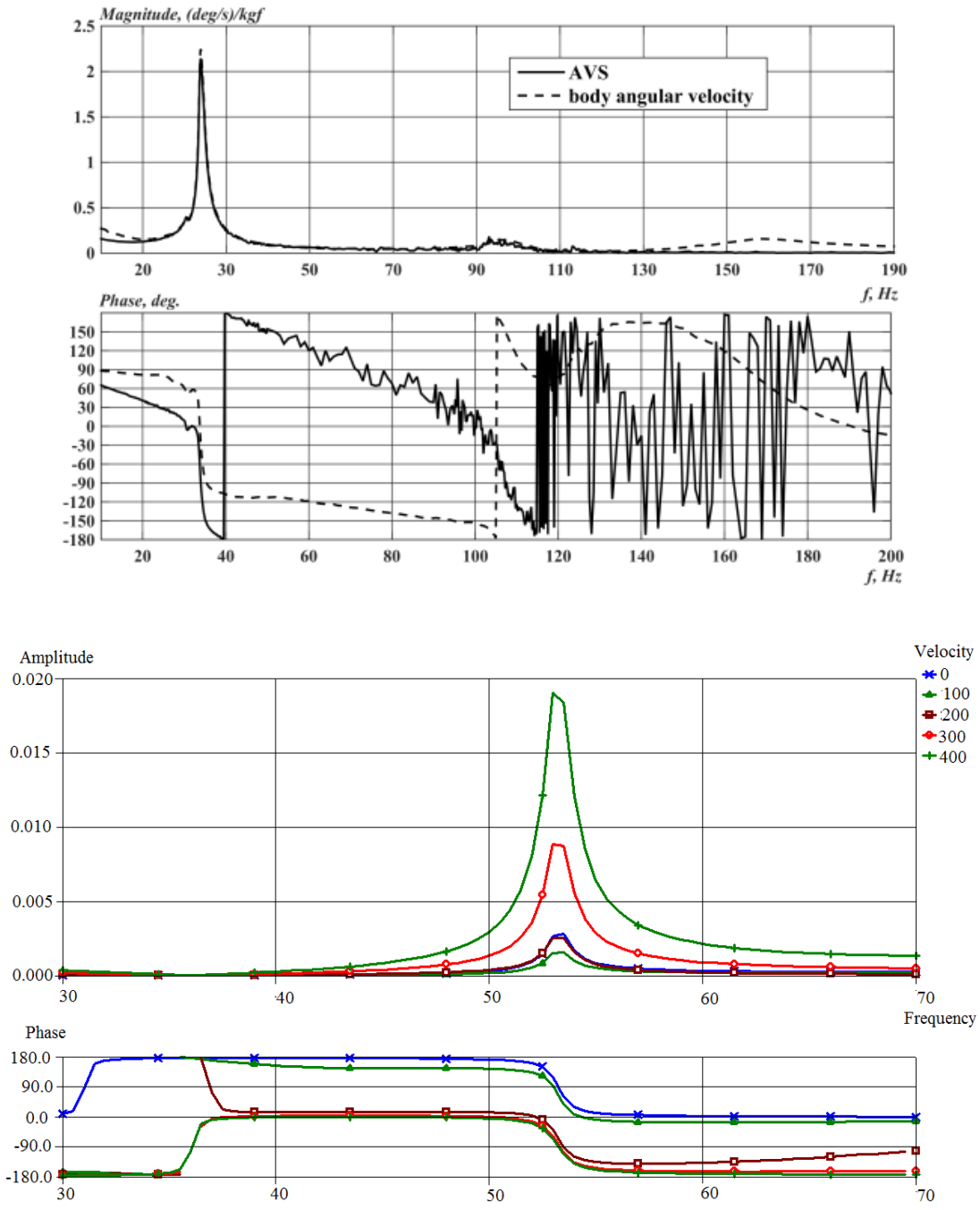

Figure 9: Body FRF in CS sensors section from force applied to the fin rotation axis

In case of 4 actuation system input signals recorded with AVS, LAS or both signals at the same time, it is necessary to apply a procedure for forming the algebraic sum of the four signals with the correct signs. This is due to the unavailability of the FRF values θ, ψ and γ (control signals for pitch, yaw and roll channales), which "exist" only within the CS program.

These values for FRF computation (from force to control fin rotation) for one channel should be multiplied by one of corresponding pairs of actuation system FRF's (Figure 6) or by averaged FRF's across all the actuators, Figure 11.

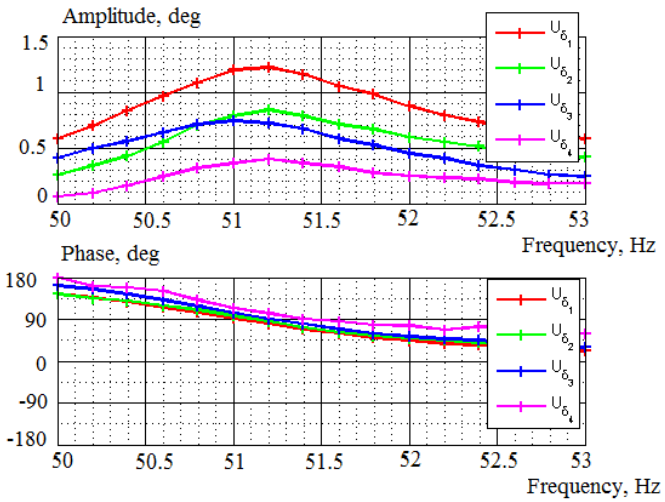

Figure 10: Body FRF from excitation force to actuation system inputs (for the angular velocity circuit)

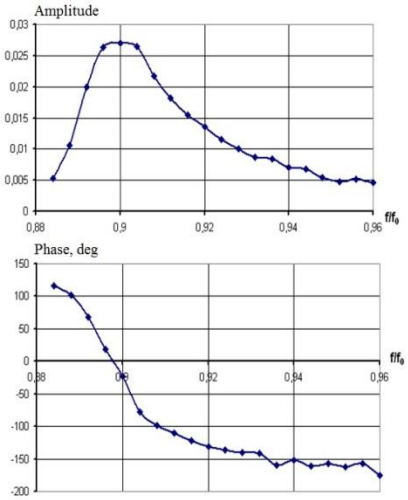

Figure 11: FRF of the "averaged control fin" divided by force on body

6 EVALUATION OF STABILITY, LIMIT CYCLES

Operating area of UFV is presented as example by function of two parameters – Mach number and altitude (H), Figure 12. The right boundary corresponds to the maximum dynamic pressure, the left boundary corresponds to the possible initial conditions, the lower horizontal line is close to H=0, though slightly higher. For a flutter computation two areas are interesting: subsonic region near the M=1 and supersonic region close to the maximum dynamic pressure. The latter is caused by small quantities of the Strouhal number for a UFV which means small influence of the aerodynamic damping.

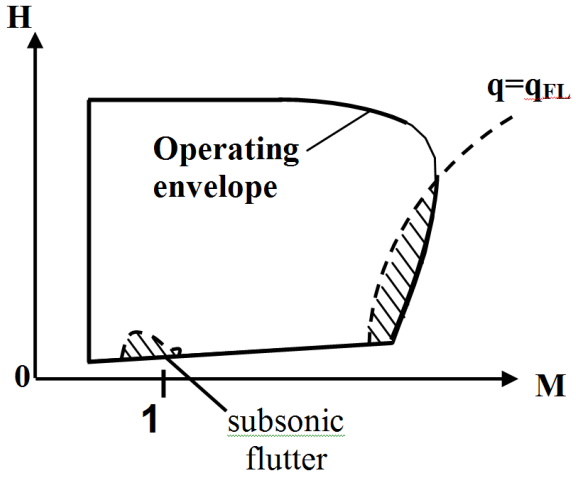

Figure 12: UFV operating area

To estimate the stability boundary of elastic UFV-CS loop, it is important to define a criterion depending on the K (product of coefficients of adaptation):

$$\max[q \cdot K(q, M) \cdot C_y^{\alpha}(M)] \tag{8}$$

Its maxima may not belong to the line of maximum dynamic pressure, Figure 13. It is necessary to select from two circuits (AVS or LAS) by more significant one (depending on influence on stability margins).

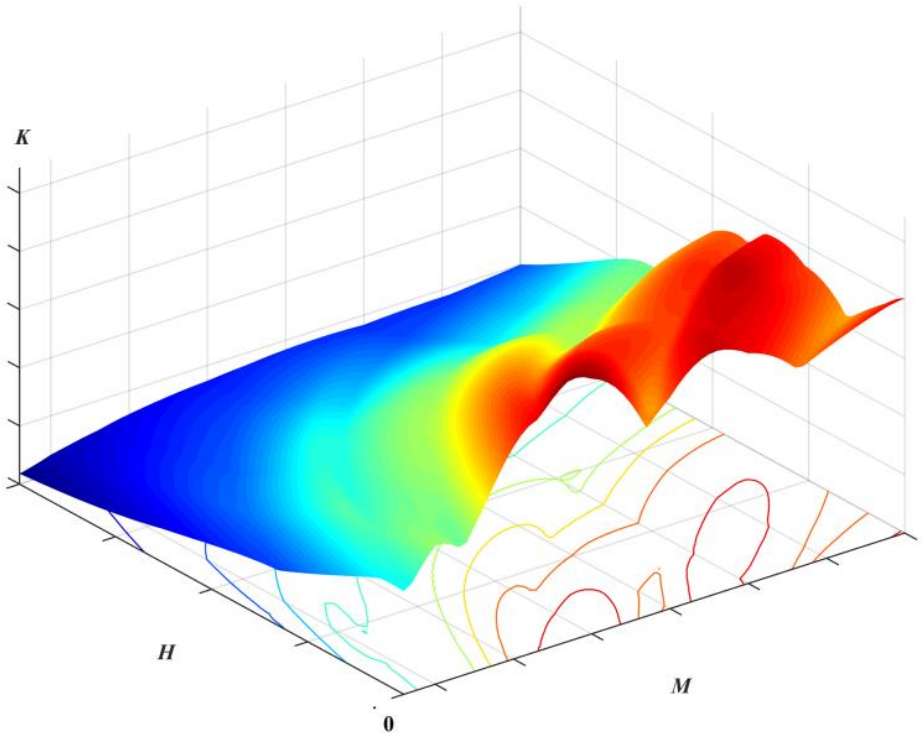

Figure 13: Value of the criterion in the UFV application area

For the selected flight regime (number of M and dynamic pressure), considering the independence of CS channels, it is necessary to obtain the FRF of circuit part from force (F) applied to body (at axis of control fin rotation) to δ_{fin} – fin deflection as the output value, or as the ratio δ_{fin}/F. Let us introduce the notations:

$$K^{B\omega} = \omega_z/F;\ K^{Bn} = n_y/F;\ K^{C\omega} = \delta^{D\omega}/F;\ K^{Cn} = \delta^{Dn}/F \tag{9}$$

where $K^{B\omega}$ and K^{Bn} – FRF of the body, $K^{C\omega}$ and K^{Cn} – frequency FRF calculated with sensors and body, $\delta^{D\omega}$ and $\delta^{D\omega}$ – inputs of each of 4 actuators at the measurement, respectively, in the AVS circuit (indices ω) or LAS (indices n). Once the adaptation coefficients $K^{\omega m}$, K^{nm} are set and their values for the considered regime are K^{ω} and K^{n} during the measurement, then correction factors for FRF of the actuator input must be introduced . With their introduction it can be summarized with computed FRF, as noted above, to obtain control signals θ, ψ and γ and then multiplied by K^{D} – to obtain FRF of the actuator

$$\delta_r/F = \theta K^D;\ \theta = (K^{C\omega}K^{\omega}/K^{\omega m} + K^{Cn}K^{n}/K^{nm});\ K^D = \delta_r/\delta^D \tag{10}$$

where δ^D is the sum of actuator input signals.

The only part to get the FRF of complete open-loop is aerodynamic ratio (estimated force F^A on one control by one degree rotation):

$$F^A = qSC_y^\alpha(M). \tag{11}$$

Thereby stability boundary is defined by relations valid for the FRF:

$$\mathrm{Re}(\theta K^D F^A) = 1; \mathrm{Im}(\theta K^D F^A) = 0 \tag{12}$$

The simplest quasi-linear estimation of the amplitudes of limit cycles should be set by the value of a predetermined limits of angular velocity in the CS algorithm, $(\dot{\delta}_{fin})_{max}$. If ω_0 is an estimated frequency of auto-oscillation by criterion (9), the amplitude of the control fin oscillations will be obviously equal to

$$\delta_0 = (\dot{\delta}_r)_{max}/\omega_0 \tag{13}$$

In stand measurements (ref. (6)) the value $K^{Bn} = n_y/F$ is measured, the acceleration in the body section of CS sensors (amplitude of the limit cycle) is

$$(n^y)_0 = (K^{Bn})_0 (F^A)_0 \delta_0, \tag{14}$$

where index 0 relates to auto-oscillations.

The stability of the limit cycle is determined by, for example, the shape of AR magnitude of open loop at the oscillation frequency. It is practically identical to shape of the loop characteristics (with the aerodynamic forces excluded) shown in Fig. 11.

This dependence is shown on Fig. 14, with arrows showing amplitude increasing and decreasing. It can be seen that there is an unstable limit cycle, at the lowest amplitude. Besides there is a stable limit cycle, with restrictions (in case of surpassing restrictions or their absence). Stable oscillations occur with the higher amplitude of the corresponding boundary of stability [6]. In the presence of restrictions with lower amplitude (dashed line in Figure 14), they will correspond to auto-oscillations.

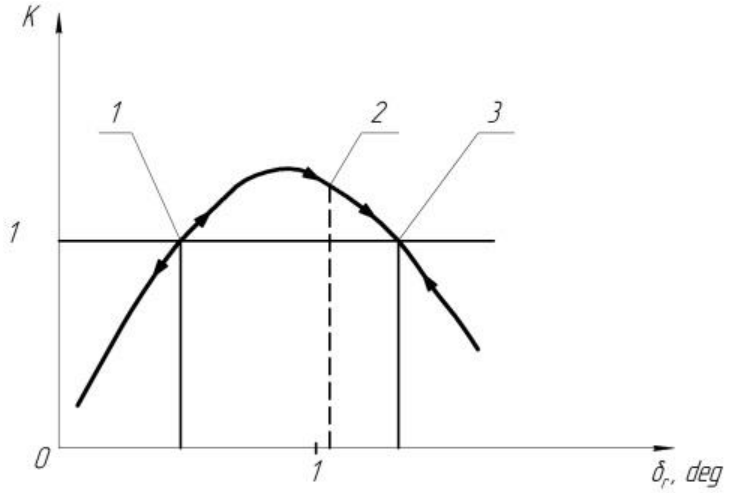

Figure 14: Limit cycles of oscillation: 1 – unstable; 2 – stable, with limitations;
3 - stable, without limitations; K – stability boundary

In the case of small stability margins it is necessary to make more accurate study of the stability of computational and experimental evaluations. It can be carried out in several directions. One of directions is aerodynamic research. Since the derivative $C_y^{\alpha}(M)$ itself occurs as a factor in the expression for the stability boundary (9), its precise estimation is crucial, for example through test evaluations using stationary tests in wind tunnels or by numeric simulation with variation of boundary conditions to clarify the impact of interference, or otherwise.

Aerodynamic effects on the body can influence on the stability boundaries, especially of it nose fairing, as well as accounting of the forces of aerodynamic damping.

The discrepancy of electromechanical actuator properties is evaluated by measuring data from multiple actuation units, with 4 actuators each, which can be not always possible.

Interference of channels caused by the previously mentioned asymmetry of the elastic-mass characteristics of the body [7] may in some cases require significant correction. One option of accounting interference, based on a linear combination of the experimental FRF of different channels is described in the paper [8].

Another option may consist in solution of the spatial problem of vibrations in the plane inclined at some angle to the control plane, that is, problem of simultaneous vibrations in two control channels. Traditionally, multi-loop system stability problem is reduced to one after one analysis of each open loop circuit and its closure.

A separate issue is the compliance of an actuator. Solution of this issue is possible to be done by computation, but so far is very approximate. The more authentic response is provided by experiment with electromechanical simulation of aerodynamic forces (EMM), as shown in Figs. 15, 16 [9]. Due to the small, in some cases, allowed time of continuous operation of electromechanical actuation system, measurement with EMM has to be carried out at the most dangerous regimes (with small stability margins). Also, if necessary, by means of EMM it is possible to investigate the characteristics of limit cycles.

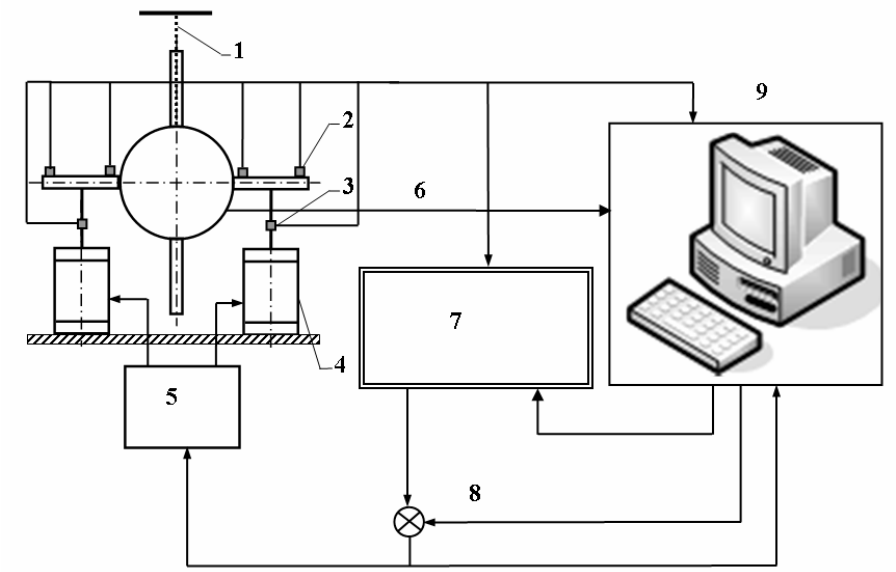

Figure 15: Simulation of elastic oscillations in flight (EMM) and actuator FRF in stream: 1 - elastic suspension, 2 - accelerometers, 3 - force sensors, 4 - exciters, 5 - power amplifiers, 6 - CS control voltage, 7 – special real-time processing unit, 8 - external excitation, 9 – experiment control system

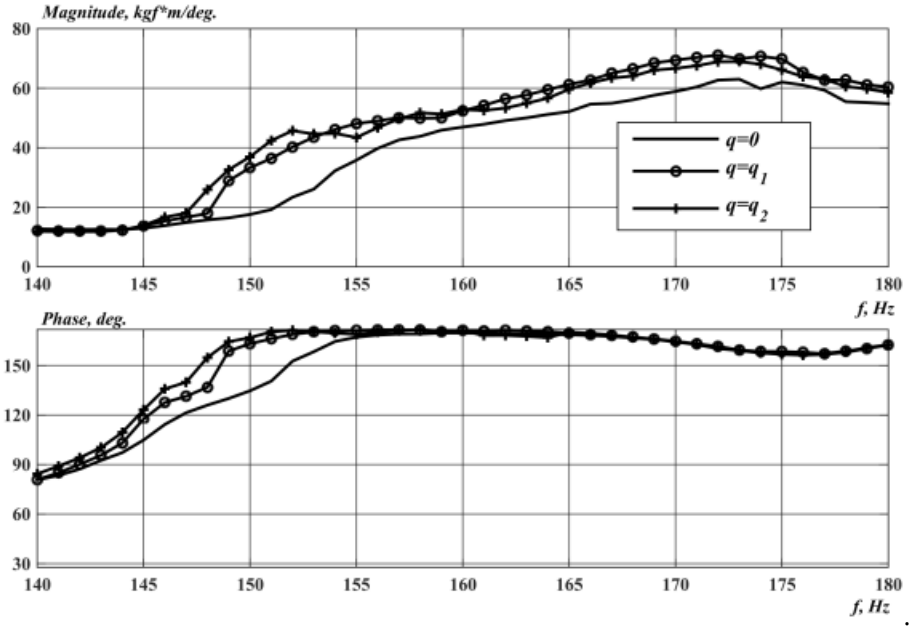

Figure 16: Actuator dynamic stiffness FRF in “stream” at some dynamic pressures

7 CONCLUSION

The task of preventing dangerous auto-oscillations in UFV in flight is solved by combination of computational and experimental methods.

Features of UFV with electromechanical actuator require a special approach.

GVT results are used to correct accuracy of the computational dynamic models.

Stability margin of elastic UFV-CS loop are evaluated by frequency criteria using data from the experimental works.

The presented research experience further the preventing of dangerous auto-oscillations of UFV in flight.

8 REFERENCES

[1] Bushgens, G. S. and Dmitriev, V. G., Aeroelasticity, Engineering Encyclopedia, Aircraft and Rotorcraft, Aerodynamics, Flight Dynamics, and Strength, *Monograph V. IV-21*, Moscow: Mashinostroenie, 2002 (in Russian).

[2] Ishmuratov F.Z., Karkle P.G., Popovski V.N. Experience and research TsAGI in aeroelasticity of aircrafts. *Proceedings of TsAGI,* 1998. № 2631. p. 103 – 113.

[3] Parafes S.G., Smyslov V.I. В.И. Methods and means of providing aeroelastic stability of unmanned aerial vehicles. – M.: MAI-PRINT Publishing house, 2013, 174 с.

[4] S.F. Alferov, V.I. Dovbischuk, V.N. Popovski, B.N. Smirnov. Experience of using frequency method in studies aeroservoelasticity. *Proceedings of TsAGI*. 2014, №2738, p 225-244.

[5] Bykov A.V., Kondrashev G.V., Parafes S.G., Turkin I.K. Research experience of properties of electrical actuator of control fin of UAV by means of electrical-mechanical simulation of aerodynamic forces, *Aerospace instrumentation*. 2015, №1, стр. 46-52.

[6] Teodorchic K.F. Auto oscillations system. M.: Gostehizdat, 1952

[7] Bykov A.V., Smyslov V,I. Investigation of maneuverable missile flutter considering principal planes of oscillations *149 Report IF-149. Presented at the International Forum on Aeroelasticity and Structural Dynamics*, Seattle United States, June 21-25, 2009.

[8] A. G. Narizhny, V.I. Smyslov, S. I. Sychev. Aeroelastic stability research of a cross shaped flying vehicle, *TsAGI Science Journal*, 44 (6): 885-909 (2013)

[9] Petr G. Karkle and Vsevolod I. Smyslov. Electromechanical simulation method in dynamic aeroelasticity – usage experience and future trends. *Report IF-025. Presented at the International Forum on Aeroelasticity and Structural Dynamics*, Stockholm, Sweden, June 18-20, 2007.

Copyright Statement